

Chemical Sensing using Graphene-based Surface-Acoustic-Wave Sensor

Satoshi Okuda^{1,2}, Takao Ono¹, Yasushi Kanai¹, Masaaki Shimatani², Shinpei Ogawa², Takashi Ikuta^{1,3}, Koichi Inoue¹, Kenzo Maehashi^{1,3} and Kazuhiko Matsumoto¹

¹ The Institute of Scientific and Industrial Research, Osaka Univ.
8-1 Mihogaoka, Ibaraki, Osaka 567-0047, Japan

Phone: +81-6-6879-8412 E-mail: okuda11@sanken.osaka-u.ac.jp

² Advanced Technology R & D Center, Mitsubishi Electric Corp.
8-1-1 Amagasaki, Hyogo 661-8661, Japan

³ Institute of Engineering, Tokyo Univ. of Agriculture and Technology
2-24-16 Nakacho, Koganei, Tokyo, 184-8588, Japan

Abstract

A graphene surface acoustic wave (G-SAW) device has been developed and applied as a chemical sensor. When a SAW propagates on graphene, carriers in graphene are transported by the SAW. This is termed the acoustoelectric current (I_A). In this research, the top-gate voltage dependence of I_A was investigated by employing a solution gate. In addition, pH sensing using the G-SAW device was performed. It was demonstrated that the G-SAW sensor has a higher sensitivity than a conventional graphene field-effect transistor based sensor.

1. Introduction

The interaction between a surface acoustic wave (SAW) and low-dimensional electron systems (LDESs), such as two-dimensional electron gases (2DEGs) in GaAs/AlGaAs heterostructures [1], carbon nanotubes [2], and graphene [3] has been examined in earlier research. Carriers in LDESs can be trapped or transported by the SAW because a SAW, which is a mechanical wave induced on a piezoelectric crystal, is accompanied by a potential wave. Recently, acoustoelectric current (I_A) flows in graphene induced by a SAW have attracted attention [3-4]. However, I_A has not been applied in field-effect transistors (FETs) because most previous studies have been conducted in air where back-gate voltage cannot be applied. In this research, we fabricated a solution-gated G-SAW device to investigate the gate-voltage response of I_A in buffer solution and to demonstrate the potential for pH sensing.

2. Experimental Procedure

A schematic illustration of the fabricated G-SAW sensor is given in Fig. 1. The single-layer graphene was transferred to the center of a 36° YX LiTaO₃ substrate. Because the LiTaO₃ substrate generates a shear horizontal (SH) SAW, the energy of the SAW is not diminished by the presence of solution. Therefore, the device is suitable for uses as a SAW-based solution sensor. Source and drain electrodes were formed on the graphene, and interdigital transducers (IDTs) were placed at both ends of the substrate. All electrodes, composed of Ni/Au of thickness 10/30 nm, were

fabricated by electron-beam evaporation. Silicone rubber was attached around the graphene, and buffer solution was dropped into the cavity. An electrolyte gate voltage (V_{EG}) was applied from a Ag/AgCl reference electrode.

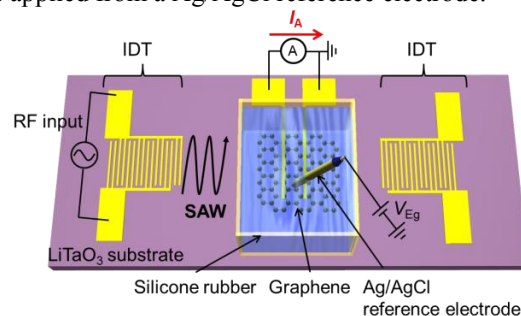


Fig. 1 Schematic of graphene SAW sensor.

3. Results and discussion

Fig. 2(a) shows the I_A - V_{EG} characteristics for the device in phthalate buffer solution at pH 4.1 when the input frequency to the IDT was increased from 110 MHz to 150 MHz in steps of 0.1 MHz. An I_A was induced around 130 MHz, which is the central frequency (f_0) determined by the period of the IDT and velocity of the SAW, and almost no I_A flows outward from f_0 . This result indicates that the SAW, which propagates on the LiTaO₃ substrate, can transport carriers in graphene in the solution phase. Fig. 2(b) shows the I_A - V_{EG} characteristics extracted at 129.9 MHz in Fig. 2(a). The flow direction of I_A was switched when crossing $V_{EG} = 80$ mV, which corresponds to the Dirac point of graphene, because the major carriers in graphene under each V_{EG} were transported by the SAW. The I_A also revealed that there were positive and negative peak values. The position where I_A reaches a maximum value is determined by the ratio of the conductivity of graphene to the conductivity of the SAW [4-5]. That is, when the carrier density of graphene is larger than the SAW conductivity, the efficiency of carrier transport by the SAW is decreased.

Next, the pH response of I_A was investigated. The pH was increased from 5.71 to 6.99 and the I_A - V_{EG} characteristics were measured. To control the pH in the buffer solution, the buffering effect between NaH₂PO₄ and Na₂HPO₄ was used. The peak shift of the hole current is shown in Fig. 3(a). The

peak was shifted in a positive direction as the pH of the buffer solution increased. Fig. 3(b) shows the pH dependence of V_{EG} when the hole current was at its maximum value (25.2 mV/pH). As the hydrogen ion content decreased, the hole density of graphene increased, hence the $I_{\text{A}}-V_{\text{EG}}$ characteristics shifted in a positive direction.

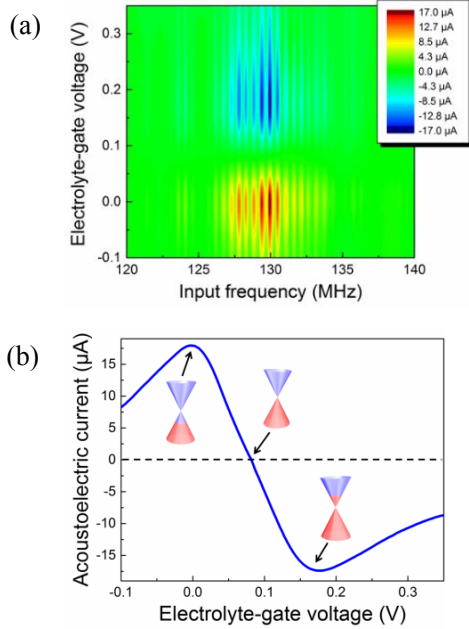


Fig. 2 (a) Contour map of I_{A} in phthalate buffer solution as a function of V_{EG} and input frequency to the IDT. (b) $I_{\text{A}}-V_{\text{EG}}$ characteristics at the input frequency of 129.9 MHz.

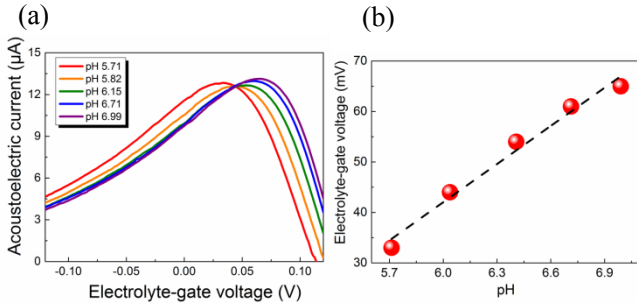


Fig. 3 (a) $I_{\text{A}}-V_{\text{EG}}$ characteristics in solution for pH range 5.71 to 6.99. (b) the pH dependence of V_{EG} for the hole current peak of I_{A} .

Finally, a comparison of pH sensitivity between a G-SAW sensor and a G-FET sensor was performed. Sensitivity is defined as $\delta I / I$, where δI is the current change resulting from the change in amount of hydrogen ions and I is the background current.

In this experiment, the same sample was used, and the G-FET mode and G-SAW mode were switched by applying a V_{D} of 20 mV to the G-FET and a V_{D} of 0 V with an RF signal to the G-SAW. The pH was increased from 5.71 to 6.99 and the current change from the initial state was measured. In the G-FET mode, the δI was typically at a maximum when the transconductance of the G-FET was at a

maximum. Therefore, δI of the G-FET sensor was measured at $V_{\text{EG}} = 0$ V, which is the maximum point of transconductance. In contrast, the G-SAW sensor was measured at $V_{\text{EG}} = 113$ mV which is around the Dirac point since I_{A} in the initial state can also be made 0 A. As shown in Fig. 4, as the pH was changed from 5.71 to 6.99, the drain current increased to 1.05 times the initial current for the G-FET mode. In contrast, for the G-SAW mode the I_{A} increased to 86 times the initial amount. Because the initial current of the G-SAW is readily controlled by adjusting V_{EG} , the G-SAW device exhibits higher sensitivity and lower power consumption than a conventional G-FET sensor.

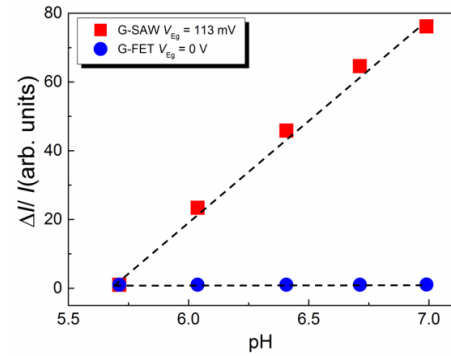


Fig. 4 Sensitivity comparison of the G-SAW and the G-FET to changes in pH of the buffer solution.

4. Conclusions

We have demonstrated the acoustoelectric effect with graphene in solution. It was found that the $I_{\text{A}}-V_{\text{EG}}$ behavior of the G-SAW sensor has different transfer characteristics than the ambipolar characteristics of the conventional G-FET device. The pH response of the G-SAW sensor was also investigated. Because I_{A} can be made 0 A by adjusting V_{EG} , the G-SAW sensor exhibits higher sensitivity and lower power consumption. Therefore, the G-SAW sensor is promising candidate for chemical and biological sensing platform.

Acknowledgements

The authors acknowledge financial support from JST CREST Grant Number JPMJCR15F4, Japan, from Innovative Areas “Molecular Architectonics: Orchestration of Single Molecules for Novel Functions” (No. 25110007) through the Ministry of Education, Culture, Sports, Science and Technology of Japan (MEXT), from a Management Expense Grant for National University Corporations from MEXT, and from a Grant-in-Aid for Young Scientists B (No.15K17679) and Scientific Research B (No. 15H03986) from the Japan Society for the Promotion of Science (JSPS).

References

- [1] A. Wixforth et al., Phys. Rev. B **40** (1989) 7874.
- [2] J. Ebbecke et al., Phys. Rev. B **70** (2004) 233401.
- [3] V. Miseikis et al., Appl. Phys. Lett. **100** (2012) 133105.
- [4] L. Bandhu et al., Appl. Phys. Lett. **103** (2013) 133101.
- [5] S. Okuda et al., Appl. Phys. Express **9** (2016) 055104.